Defence Research and Development Canada
Recherche et développement pour la défense Canada

DEFENCE R&D DÉFENSE

Tracking performance of multiple-input multiple-output radar for accelerating targets

Peter W. Moo
Defence Research and Development Canada – Ottawa

Zhen Ding
Defence Research and Development Canada – Ottawa

Defence R&D Canada - Ottawa

Technical Memorandum
DRDC Ottawa TM 2012-167
October 2013

Canada

Tracking performance of multiple-input multiple-output radar for accelerating targets

Peter W. Moo
Defence Research and Development Canada – Ottawa

Zhen Ding
Defence Research and Development Canada – Ottawa

Defence Research and Development Canada – Ottawa
Technical Memorandum
DRDC Ottawa TM 2012-167
October 2013

Abstract

Multiple-input multiple-output (MIMO) radar utilizes orthogonal waveforms on each transmit element to achieve virtual aperture extension. Compared to a directed beam radar, MIMO radar has increased Doppler resolution due to longer integration times. However, the requirement for longer integration times can also cause target returns to be spread over multiple range-Doppler bins, which decreases probability of detection. This technical memorandum derives an analytical expression for probability of detection that explicitly accounts for range-Doppler migration. The effect of target velocity, target acceleration and integration time on range-Doppler migration is analysed. A framework for velocity and acceleration compensation and step sizes for full and partial compensation are proposed. Single-target track completeness and track accuracy are computed for four configurations: directed beam radar, MIMO radar with full compensation, MIMO radar with partial compensation, and uncompensated MIMO radar. Results indicate that compensation is required to prevent degraded probability of detection as target velocity and acceleration increase. Full compensation mitigates the effects of range-Doppler migration but requires additional computational complexity. The use of partial compensation reduces computational complexity requirements but has diminished tracking performance due to coasting over missed measurements.

Résumé

Les radars entrée multiple sortie multiple (MIMO) utilisent des formes d'onde orthogonales sur chaque élément émetteur afin de produire une extension virtuelle de leur ouverture. Un radar MIMO a une résolution Doppler plus grande qu'un radar à faisceau dirigé en raison de l'accroissement des temps d'intégration. Cette augmentation des temps d'intégration peut cependant faire en sorte que les échos des cibles s'étendent sur de multiples cellules distance-Doppler, ce qui diminue la probabilité de détection. Le présent document technique développe une expression analytique de la probabilité de détection qui tient explicitement compte de la migration de cellule distance-Doppler. Les effets de la vitesse et de l'accélération de la cible ainsi que du temps d'intégration sur la migration distance-Doppler est analysée. Un cadre de compensation de la vitesse et de l'accélération est proposé ainsi que des grandeurs d'intervalle pour une compensation complète et partielle. L'intégrité et la précision des pistes à une seule cible sont calculées pour quatre configurations : radar à faisceau dirigé, radar MIMO avec compensation complète, radar MIMO avec compensation partielle et radar MIMO sans compensation. Les résultats indiquent qu'une compensation est nécessaire pour empêcher la dégradation de la probabilité de détection lorsque la vitesse et l'accélération de la cible augmentent. La compensation complète réduit les effets de la migration distance-Doppler, mais elle nécessite une complexité de calcul accrue. L'utilisation d'une compensation partielle réduit la puissance de calcul nécessaire, mais elle diminue le rendement de poursuite en

raison de mesures manquées qui obligent le radar à avancer à l'aveuglette.

Executive summary

Tracking performance of multiple-input multiple-output radar for accelerating targets

Peter W. Moo, Zhen Ding; DRDC Ottawa TM 2012-167; Defence Research and Development Canada – Ottawa; October 2013.

Background: Multiple-input multiple-output (MIMO) radar uses multiple transmitters and multiple receivers, and has enhanced flexibility and complexity compared to a traditional phased array radar, also known as a directed beam radar. The additional degrees of freedom available to a MIMO radar enable the use of omnidirectional search modes and transmit beamsteering on receive. Because MIMO radar transmits orthogonal waveforms, it requires longer integration times to compensate for reduced antenna gain, compared to a directed beam radar. The longer integration times increase Doppler resolution but also enhance the severity of range-Doppler migration for a target with high velocity or acceleration. In this technical memorandum, the tracking performance of MIMO radar and that of directed beam radar are compared for accelerating targets. The longer integration times are explicitly taken into account.

Principal results: An analytical expression for probability of detection that accounts for range-Doppler migration is derived. The effect of target velocity, target acceleration and integration time on range-Doppler migration is analysed. Conditions to limit migration effects are determined, based on radar and target parameters. When these conditions are not satisfied, it is proposed that velocity and acceleration compensation be performed. The effect of full and partial compensation techniques is modeled, where partial compensation techniques have reduced computational complexity. A comparison of single-target tracking performance is carried out using the derived expression for probability of detection, an Integrated Multiple Model (IMM) tracker, and a Monte Carlo simulation method. For an accelerating target, track completeness and track accuracy are computed for four configurations: directed beam radar, MIMO radar with full compensation, MIMO radar with partial compensation, and uncompensated MIMO radar. For the examples considered, uncompensated MIMO radar has reduced probability of detection and track completeness due to range-Doppler migration. For targets with 0.3 m/s^2 acceleration or less, MIMO radar with full compensation achieves the same track completeness and track accuracy as directed beam radar. For a target with 0.9 m/s^2 acceleration, MIMO radar with full compensation achieves higher initial track accuracy than directed beam radar, due to higher velocity estimation accuracy. MIMO radar with partial compensation suffers from degraded track accuracy due to missed detections which force the tracker to coast.

Significance of results: The analytical expressions derived in this memorandum enable the explicit calculation of detection performance when designing a radar system. In particular, the trade-offs between the use of a phased array configuration and a MIMO configuration can be quantified for varying radar system parameters and target characteristics. An approach was proposed to mitigate some adverse effects of the longer integration time required for MIMO radar, and the resulting system performance was modeled. These modelling results help to characterise the tracking performance and signal processing complexity of a MIMO radar system.

Future work: The expressions derived in this technical memorandum assume ideal orthogonality between waveforms. Future work shall study the design and implementation of orthogonal waveforms for MIMO radar. In practice, it may not be possible to achieve perfect orthogonality between waveforms, which may degrade MIMO radar performance. Also, this study considered a MIMO radar configuration where all array elements are used as transmitters and receivers. In the future, alternative MIMO configurations should be examined, with respect to orthogonal waveform requirements, detection and tracking performance, and computational complexity requirements.

Sommaire

Tracking performance of multiple-input multiple-output radar for accelerating targets

Peter W. Moo, Zhen Ding ; DRDC Ottawa TM 2012-167 ; Recherche et développement pour la défense Canada – Ottawa ; octobre 2013.

Introduction : Les radars entrée multiple sortie multiple (MIMO) emploient des récepteurs et des émetteurs multiples ; ils sont plus souples et plus complexes que le radar à réseau à commande de phase traditionnel, quon appelle également un radar à faisceau dirigé. Les degrés de liberté supplémentaire du radar MIMO lui permettent dutiliser des modes de recherche omnidirectionnels et de la formation de faisceau démission à la réception. Comme un radar MIMO émet des formes donde orthogonales, il exige un temps dintégration plus long pour compenser le gain dantenne réduit par rapport à un radar à faisceau dirigé. Cet allongement du temps dintégration augmente la résolution Doppler, mais il accentue la migration distance-Doppler des cibles dont la vitesse ou laccélération est élevée. Dans le présent document technique, le rendement de poursuite de cibles en accélération dun radar MIMO est comparé à celui dun radar à faisceau dirigé en tenant explicitement compte de laugmentation du temps dintégration.

Résultats : On a développé une expression analytique de la probabilité de détection qui tient compte de la migration distance-Doppler. Leffet de laccélération de la cible, de sa vitesse et du temps dintégration sur la migration distance-Doppler est analysée. Les conditions nécessaires pour limiter les effets de migration sont déterminées en fonction des paramètres du radar et de la cible. Lorsque ces conditions ne sont pas remplies, on propose dappliquer une compensation de laccélération et de la vitesse. Leffet de techniques de compensation complète ou partielle est modélisé, les techniques de compensation partielle ayant une complexité de calcul réduite. Une comparaison de la poursuite dune seule cible est faite au moyen de lexpression analytique de la probabilité de détection, dun système de poursuite à modèles multiples à interactions (IMM) et dune méthode de simulation Monte-Carlo. Pour une cible en accélération, on calcule lintégrité et la précision de poursuite pour quatre configurations : radar à faisceau dirigé, radar MIMO avec compensation complète, radar MINO avec compensation partielle et radar MIMO sans compensation. Pour les exemples étudiés, le radar MIMO sans compensation a une probabilité de détection et une intégrité de poursuite réduites en raison de la migration distance-Doppler. Pour les cibles ayant une accélération de 0,3 m/s^2 ou moins, le radar MIMO avec compensation complète permet dobtenir la mme intégrité et précision de poursuite que le radar à faisceau dirigé. Pour une cible ayant une accélération de 0,9 m/s^2, le radar MIMO à compensation complète obtient une meilleure précision de poursuite initiale que le radar à faisceau grce à son évaluation de la vitesse plus précise. Le radar MIMO à compensation partielle souffre

dune moins bonne précision de poursuite en raison de détections manquées qui forcent le radar à avancer à laveuglette.

Portée : Les expressions analytiques développées dans le présent document permettent un calcul explicite de la performance de détection au cours de la conception dun système radar. Plus particulièrement, elles permettent de quantifier les compromis quimpose lutilisation dune configuration à réseau à commande de phase par rapport à une configuration MIMO pour divers paramètres radar et caractéristiques de cible. Une approche a été proposée pour réduire certains des effets nuisibles du temps dintégration plus long quexige le radar MIMO ; la performance du système résultant a été modélisée. Ces résultats de modélisation contribuent à caractériser la performance de poursuite et la complexité du traitement de signal dun système radar MIMO.

Recherches futures : Les expressions développées dans le présent rapport supposent une orthogonalité idéale entre les formes d'ondes. Des travaux futurs étudieront la conception et la mise en oeuvre d'un radar MIMO à formes d'onde orthogonales. En pratique, il pourrait très impossible d'obtenir une orthogonalité parfaite des formes d'onde, ce qui pourrait réduire la performance du radar MIMO. La présente étude a également porté sur une configuration ou tous les éléments du réseau servent à la fois d'émetteurs et de récepteurs. Par la suite, d'autres configurations de radar MIMO devraient tres étudiées en ce qui a trait à l'exigence de formes d'onde orthogonales, du rendement de détection et de poursuite et de la complexité de calcul.

Table of contents

List of figures

List of tables

1 Introduction

Multiple-input multiple-output (MIMO) radar uses multiple transmitters and multiple receivers, and has enhanced flexibility and complexity compared to a traditional phased array radar, also known as a directed beam radar. In this work, attention is focused on coherent MIMO radar, where the transmitters and receivers are co-located. Multiple transmitters and receivers enable the use of omnidirectional search modes and transmit beamsteering on receive [1], [2]. MIMO operation requires the use of orthogonal waveforms on transmit and increased signal processing on receive. The transmission of orthogonal waveforms reduces antenna gain, which, compared to a directed beam radar, necessitates longer integration times to maintain the same energy on target. Greater Doppler resolution is achieved by MIMO radar due to longer integration times. However, longer integration times can also cause target returns to be spread over multiple range-Doppler bins, which decreases probability of detection. This technical memorandum compares the tracking performance of MIMO radar and directed beam radar. As an intermediate step, an expression for probability of detection that explicitly accounts for range-Doppler migration is derived. The effect of target velocity, target acceleration, and integration times on range-Doppler migration is analysed, and methods for full and partial compensation of velocity and acceleration are proposed. These results are then used to carry out a tracking performance comparison and characterise the advantages and limitations of tracking accelerating targets with MIMO radar.

Rabideau [3] conducted a tradeoff analysis for MIMO radar and directed beam radar by minimising an objective function that describes the relationship between performance and cost. In [4], directed beam radar and MIMO radar were compared for non-Doppler envelope detection of high-velocity targets. Target tracking resolution for MIMO radar was described with respect to ambiguity functions in [5]. Multiple target tracking for MIMO radar was considered in [6], where target localisation performance was analysed. In this technical memorandum the tracking performance of directed beam radar and MIMO radar are compared by computing probability of detection whilst explicitly accounting for range-Doppler migration. Fourier spectrum analysis has formed the basis for previous characterisation of range-Doppler migration [7], [8]. Here range-Doppler migration is accounted for by computing the fractional received power in all range-Doppler bins.

This technical memorandum is organised as follows. Section 2 presents the tracking problem that is addressed in this work. Section 3 computes the antenna patterns for a directed beam radar and a MIMO radar. Section 4 derives an expression for probability of detection that accounts for the range-Doppler migration of moving targets. In Section 5 the effects of range-Doppler migration are analysed for varying values of target velocity and acceleration and for both directed beam and MIMO radar modes. Section 6 proposes full and partial compensation schemes to mitigate range-Doppler migration. In Section 7 the tracking performance of directed beam and MIMO radar modes are compared. Finally, conclusions are

presented in Section 8.

2 Problem description

The radar is a linear antenna array with M transmit/receive elements and is operated in one of two modes. In Directed Beam mode, each element transmits the same waveform with a phase shift to steer the beam. In MIMO mode, each element transmits a distinct orthogonal waveform, through the use of orthogonal frequency division multiplexing or time division multiplexing. Ideal orthogonality between waveforms is assumed. In both modes, the return signal is received on all elements. Also, the radar carries out Doppler processing in both modes. When comparing the modes, the same physical aperture length will be used.

The goal of this technical memorandum is to compare the single-target tracking performance of Directed Beam mode and MIMO mode. Detection is assumed to be noise-limited. In the presence of clutter, the additional degrees of freedom afforded by MIMO would likely improve detection performance. Tracking performance will be measured by evaluating two metrics: track completeness and position error, which measures track accuracy. Track completeness C is given by

$$C = \frac{\text{total time interval over which any track number is assigned to target}}{\text{total time that target is in the defined coverage area of radar}} \tag{1}$$

so that $0 \leq C \leq 1$. The coverage area is defined as the region where the signal-to-noise ratio exceeds a specified threshold. Track accuracy is measured by squared position error

$$e = \|\hat{\zeta} - \zeta\|^2,$$

where $\hat{\zeta}$ is the track position estimate and ζ is the ground truth position. In an ideal case, track completeness is one and squared position error is zero.

As shown in Section 3, the two-way radiation pattern for Directed Beam mode is equal to that for MIMO mode. As a result, the beamwidth of Directed Beam mode θ_{dir} and the beamwidth of MIMO mode θ_{MIMO} satisfy

$$\theta_{MIMO} = \theta_{dir}. \tag{2}$$

The angular estimation error of track measurements is equal for both modes.

For a fixed length array, directed beam and MIMO modes differ in two key performance characteristics, each of which affects tracking performance:

1. Doppler bin width

2. Probability of detection due to range-Doppler migration

MIMO mode transmits orthogonal waveforms which reduces transmitter gain by a factor of M relative to Directed Beam mode. Consequently, to maintain the same signal-to-noise ratio with all else being equal, MIMO mode requires a coherent processing interval (CPI) that is M times longer than that of Directed Beam mode. Since Doppler bin width is the inverse of CPI length, the Doppler bin width of Directed Beam mode Ω_{dir} and the Doppler bin width of MIMO mode Ω_{MIMO} satisfy

$$\Omega_{MIMO} = \frac{\Omega_{dir}}{M}. \tag{3}$$

Smaller Doppler bin width reduces the velocity estimation error of track measurements.

Longer integration times may have a detrimental effect on the detection of moving targets. Although the target is located in a single range-Doppler bin at the start of the CPI, the received signal may be spread over multiple range-Doppler bins. The severity of this range-Doppler migration depends on the length of the CPI and the magnitude of the velocity and acceleration of the target. Range-Doppler migration may reduce probability of detection since the effective signal-to-noise ratio (SNR) in any given range-Doppler bin is reduced. Because range-Doppler migration can significantly reduce SNR, there is a need to quantify the effect of range-Doppler migration on probability of detection. A key contribution of this technical memorandum is a closed form expression for probability of detection that explicitly accounts for range-Doppler migration. This expression is derived and presented in Section 4. The analytical expression enables a comprehensive comparison of tracking performance between Directed Beam mode and MIMO mode, where differences in Doppler bin width are also taken into account. Such a comparison is presented in Section 7.

3 Antenna Patterns

This section derives the two-way antenna radiation patterns for a linear array operating in Directed Beam mode and MIMO mode. The M-element linear array has an element pattern $F_e(\theta)$ and an array factor $F_a(\theta)$, where θ is the azimuth angle.

In Directed Beam mode, the transmit radiation pattern $G_{\mathrm{D,Tx}}(\theta)$ and the receive radiation pattern $G_{\mathrm{D,Rx}}(\theta)$ are equal, so that

$$G_{\mathrm{D,Tx}}(\theta) = G_{\mathrm{D,Rx}}(\theta) = F_e(\theta)\,F_a(\theta).$$

The two-way radiation pattern $G_{\mathrm{D},2-\mathrm{way}}(\theta)$ is given by

$$G_{\mathrm{D},2-\mathrm{way}}(\theta) = G_{\mathrm{D,Tx}}(\theta)\,G_{\mathrm{D,Rx}}(\theta) = F_e(\theta)^2\,F_a(\theta)^2.$$

In MIMO mode, each element transmits a distinct orthogonal waveform which is received on all elements. Consequently, the transmit radiation pattern $G_{\mathrm{M,Tx}}(\theta)$ is given by the element pattern,

$$G_{\mathrm{M,Tx}}(\theta) = F_e(\theta).$$

On receive, the effective array is the spatial convolution of the transmit linear array and the receive linear array [9]. Therefore, the MIMO receive array factor is the product of the Directed Beam transmit array factor and the Directed Beam receive array factor, that is, $F_a(\theta)^2$. The MIMO receive radiation pattern $G_{\mathrm{M,Rx}}(\theta)$ is then specified by

$$G_{\mathrm{M,Rx}}(\theta) = F_e(\theta)\,F_a(\theta)^2.$$

The two-way radiation pattern $G_{\mathrm{M,2-way}}(\theta)$ is given by

$$G_{\mathrm{M,2-way}}(\theta) = G_{\mathrm{M,Tx}}(\theta)\,G_{\mathrm{M,Rx}}(\theta) = F_e(\theta)^2\,F_a(\theta)^2.$$

The two-way radiation pattern for MIMO mode is equal to the two-way radiation pattern for Directed Beam mode.

4 Probability of detection with range-Doppler migration

In this section, an expression for probability of detection which accounts for range-Doppler migration is presented. To develop this expression, the range and Doppler characteristics of the target during the CPI are accounted for, and the fractional received power in each range-Doppler bin is computed.

The following parameters describe the radar.

- T is the length of the CPI, in seconds
- λ is the wavelength, in meters
- ρ is the length of the range cell, in meters

The following parameters describe the target.

- v is the target velocity at the start of the CPI, in m/s, with $v > 0$,
- a is the target acceleration (assumed constant) during the CPI, in m/s^2, with $a > 0$.

The received signal is sampled and divided into a series of range cells. In each range cell, the sampled signal is subject to Doppler processing. In each range-Doppler bin, target detection is carried out by performing threshold detection; that is, the radar must decide between two hypotheses,

$$\begin{aligned} H_0 &: z = u, \\ H_1 &: z = w + u, \end{aligned}$$

where is w the complex target return and u is zero-mean complex Gaussian noise with variance σ^2. A threshold detector can be expressed as

$$|z| \gtrless_{H_0}^{H_1} \beta,$$

where the threshold β is chosen to satisfy a specified probability of false alarm P_{fa}, that is,

$$\Pr(|u| > \beta) = P_{\text{fa}}.$$

Since the noise magnitude has a Rayleigh distribution, the threshold satisfies

$$\beta = \left(\ln P_{fa}^{-\sigma^2}\right)^{1/2}. \tag{4}$$

The width of a Doppler bin is given by $\Omega = 1/T$. The distance traveled by the target during the CPI is

$$\alpha = vT + \frac{1}{2}aT^2. \tag{5}$$

Corresponding to the initial velocity v is the initial Doppler frequency $f' = 2v/\lambda$. If $a = 0$, then the Doppler frequency is f' during the CPI. If $a \neq 0$, then the change in velocity during the CPI is given by aT, so that the Doppler frequency at the end of the CPI is $f' + (2/\lambda)aT$. Define the initial ambiguous Doppler frequency as $f = f' \mod \Omega$.

Similarly, define the initial ambiguous target range as $r = r' \mod \rho$, where r' is the target range at the beginning of the CPI. The initial ambiguous Doppler frequency f, initial ambiguous range r and their relationships to range-Doppler bins are shown in Figure 1.

To facilitate the derivation, the following terms are defined. The Doppler ratio Q_d is defined as the ratio of the change in Doppler frequency to the Doppler bin width, so that

$$Q_d = \frac{(2/\lambda)aT}{\Omega} = \frac{2}{\lambda}aT^2. \tag{6}$$

The range ratio Q_r is defined as the ratio of the distance traveled to range cell length, so that

$$Q_r = \frac{\alpha}{\rho} = \frac{vT}{\rho} + \frac{aT^2}{2\rho} = \frac{vT}{\rho} + \frac{(\lambda/4)Q_d}{\rho}. \tag{7}$$

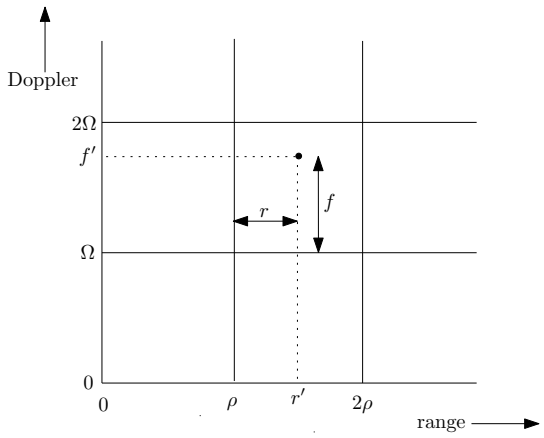

Figure 1: Illustration of initial ambiguous Doppler frequency f and initial ambiguous range r.

4.1 General form for probability of detection

For a target with non-zero velocity or non-zero acceleration, the target return may be spread over multiple range-Doppler bins. In this case, a detection is declared if the target is detected in any range-Doppler bin. The probability of detection P_d is one minus the probability that the target is not detected in any range-Doppler bin. Probability of detection is calculated by determining the total number of range-Doppler bins containing the target return and computing the fractional power located in each range-Doppler bin. Let D be the number of Doppler bins containing target returns. For Doppler bin k, let i_k be the number of range cells containing target returns. The term $c(k,n)$ specifies the fractional target return power contained in Doppler bin k and range cell n, where $1 \leq k \leq D$ and $1 \leq n \leq i_k$. Define the bin count γ as the total number of range-Doppler bins containing target returns. The bin count is given by

$$\gamma = \sum_{k=1}^{D} i_k. \tag{8}$$

In range-Doppler bin (k,n), probability of detection is given by

$$P_d = \Pr(|u + c(k,n)\, w| > \beta).$$

The envelope of the noise u and target signal $c(k,n)\, w$ has a Rician distribution [10]. Probability of detection in one or more range-Doppler bins is therefore given by the expression

$$P_d = 1 - \prod_{k=1}^{D} \prod_{n=1}^{i_k} \int_0^{\beta} \frac{2x}{\sigma^2} \exp\left(-\frac{x^2 + c(k,n)^2 y^2}{\sigma^2} \right) I_0\left(c(k,n)\, \frac{2xy}{\sigma^2} \right) dx,$$

where I_0 is a modified Bessel function of the first kind. Total SNR is given by y^2/σ^2, where y is the received target energy. In the following section, an expression for $c(k,n)$ is derived.

4.2 Derivation of fractional power

The aim of this section is to determine the time that the target spends in each range-Doppler bin. To calculate this, the time spent in each Doppler bin and in each range cell is computed independently. The time spent in each range-Doppler bin is then calculated. In the derivation that follows, the CPI is assumed to start at time zero.

The first step is to determine how many Doppler intervals the target is spread over, and the time that the target exits each Doppler interval. By definition, the initial ambiguous Doppler frequency satisfies $0 \leq f \leq \Omega$. For the last Doppler interval the exit time will be the end of the CPI, T. For Doppler intervals $1,...,D$, denote the exit times as $d(1),...,d(D)$. For all values of D, $d(D) = T$. In the following, the values of $d(1),...,d(D-1)$ are specified.

The number of Doppler intervals D is related to the Doppler ratio as follows,

$$D = \begin{cases} \lceil Q_d \rceil, & \text{if } f \leq \lceil Q_d \rceil \Omega - \frac{2aT}{\lambda} \\ \lceil Q_d \rceil + 1, & \text{otherwise} \end{cases}.$$

The operator $\lceil \cdot \rceil$ denotes the smallest integer equal to or greater than the argument. Since $d(D) = T$ for all D, only the case $D \geq 2$ needs to be considered. The velocity at the start of the first Doppler bin (and of the CPI) is $(\lambda/2)f$, and the velocity at the end of Doppler bin k is $(\lambda/2)k\Omega$. The change in velocity is given by

$$\frac{\lambda}{2}(k\Omega - f) = a \cdot d(k).$$

Therefore,

$$d(k) = \frac{\lambda}{2a}(k\Omega - f), k = 1,...,D-1.$$

The next step is to calculate S, the number of range cells over which the target return is spread, and the exit time for each range cell. The initial ambiguous target range satisfies $0 \leq r \leq \Omega$. Let $t(m)$ denote the time that the target exits range cell m, where $1 \leq m \leq S$. For all values of S, $t(S) = T$.

The number of range cells S is related to the range ratio as follows,

$$S = \begin{cases} \lceil Q_r \rceil, & \text{if } r \leq \lceil Q_r \rceil \rho - \alpha \\ \lceil Q_r \rceil + 1, & \text{otherwise} \end{cases}.$$

For $S \geq 2$ and $m = 1,...,S-1$ the target exits range cell m at time $t(m)$. At time $t(m)$, the target has traveled a distance of $m\rho - r$ since the start of the CPI. Therefore,

$$m\rho - r = vt(m) + \frac{1}{2}at(m)^2.$$

Solving the quadratic equation yields

$$t(m) = \frac{-v + \sqrt{v^2 + 2a(m\rho - r)}}{a}.$$

The exit times for the Doppler bins and range cells are specified above. Define $d(0) = 0$ and $t(0) = 0$. Recall that i_k is the number of range cells containing target returns in Doppler bin k. The term $c(k,n)$ specifies the fractional target return power contained in Doppler bin k and range cell n, where $1 \leq k \leq D$ and $1 \leq n \leq i_k$.

For Doppler bin k, define

$$\begin{aligned} x_k &= \underset{m:t(m)<d(k)}{\text{argmax}} \; t(m), \\ y_k &= \underset{m:t(m)\leq d(k-1)}{\text{argmax}} \; t(m). \end{aligned}$$

The number of range cells containing target returns in Doppler bin k is given by

$$i_k = x_k \; - \; y_k \; + \; 1.$$

The fractional target return power for the range-Doppler bin corresponding to range cell i_k in Doppler bin k is

$$c(k, i_k) = \frac{d(k) - \max[d(k-1), t(x_k)]}{T}.$$

If $i_k \geq 2$, then the values of fractional target return power for the remaining range-Doppler bins in Doppler bin k are given by

$$\begin{aligned} c(k,1) &= \frac{t(x_k + 2 - i_k) - d(k-1)}{T} \\ c(k,n) &= \frac{t(x_k + n + 1 - i_k) - t(x_k + n - i_k)}{T}, \; n = 2, 3, ..., (i_k - 1). \end{aligned}$$

This yields the general expression,

$$c(k,n) = \frac{\min\left[d(k), t(x_k + n - i_k + 1)\right] - \max\left[d(k-1), t(x_k + n - i_k)\right]}{T}, \; n = 1, ..., i_k.$$

4.3 Final expression

To summarize, the probability of detection is given by

$$P_d \;\; = \;\; 1 - \prod_{k=1}^{D} \prod_{n=1}^{i_k} \int_0^{\beta} \frac{2x}{\sigma^2} \exp\left(-\frac{x^2 + c(k,n)^2 y^2}{\sigma^2} \right) I_0\left(c(k,n) \frac{2xy}{\sigma^2} \right) dx, \qquad (9)$$

where

$$
\begin{aligned}
c(k,n) &= \frac{1}{T}\left(\min\left[d(k), t(x_k+n-i_k+1)\right] - \max\left[d(k-1), t(x_k+n-i_k)\right]\right),\ n=1,...,i_k,\\
x_k &= \underset{m:t(m)<d(k)}{\operatorname{argmax}}\ t(m),\\
y_k &= \underset{m:t(m)\le d(k-1)}{\operatorname{argmax}}\ t(m),\\
i_k &= x_k - y_k + 1,\\
S &= \begin{cases} \lceil Q_r \rceil, & \text{if } r \le \lceil Q_r \rceil \rho - \alpha \\ \lceil Q_r \rceil + 1, & \text{otherwise} \end{cases}\\
t(m) &= \begin{cases} 0, & m = 0 \\ \frac{-v+\sqrt{v^2+2a(m\rho-r)}}{a}, & 1 \le m \le S-1 \\ T, & m = S \end{cases}\\
D &= \begin{cases} \lceil Q_d \rceil, & \text{if } f \le \lceil Q_d \rceil \Omega - \frac{2aT}{\lambda} \\ \lceil Q_d \rceil + 1, & \text{otherwise} \end{cases}\\
d(k) &= \begin{cases} 0, & k = 0 \\ \frac{\lambda}{2a}(k\Omega - f), & 1 \le k \le D-1 \\ T, & k = D \end{cases},
\end{aligned}
$$

and β, α, Q_d, and Q_r are given by (4), (5), (6), and (7). The integral in (9) can be evaluated numerically. For all examples presented in this technical memorandum, it will be assumed that the initial range of the target is in the centre of a range cell, that is, $r = \rho/2$. This derivation relied on the assumption that $v > 0$ and $a > 0$. When $v < 0$ or $a < 0$, it is straightforward to modify this approach to derive a similar expression for probability of detection. Details are not provided here.

5 Analysis of range-Doppler migration

In this section, the probability of detection is analysed for varying values of target velocity and acceleration. In addition, the detection performance of MIMO radar is modelled and analysed.

5.1 Conditions to limit migration effects

Probability of detection as specified by (9) is maximized when the target return is concentrated in a single range-Doppler bin. This is the case when there is no range-Doppler migration. In the following, conditions on radar and target parameters to limit range-Doppler migration effects are proposed.

As specified in (6), the parameter Q_d measures Doppler spreading during the CPI. A reasonable condition for limiting Doppler migration is given by $Q_d \leq 0.5$. This is equivalent to the condition

$$aT^2 \leq \frac{\lambda}{4}. \tag{10}$$

Wavelength λ, target acceleration a and CPI length T should satisfy (10) to limit the effects of Doppler migration.

The parameter Q_r, as specified in (7), measures the range cell migration during the CPI. Unless $a \gg v$ it will usually be the case that $vT \gg \lambda Q_d$. As a result, the second term in (7) is usually small and does not make a significant contribution to Q_r. A reasonable condition for limiting range migration is given by $Q_r \leq 0.5$. Ignoring the second term in (7), this is equivalent to

$$vT \leq \frac{\rho}{2}. \tag{11}$$

The range cell length ρ, target velocity v and CPI length T should satisfy (11) to limit the effects of range migration. It is not possible to guarantee that range or Doppler migration will not occur. However, satisfying the conditions in (10) and (11) limits the effects of range and Doppler migration.

5.2 Comparison with Fourier spectrum analysis

Reversing the inequalities in (10) and (11) yields the conditions for which velocity and acceleration compensation should be carried out. Table 1 compares the conditions for compensation from (10) and (11), which is referred to as the range and Doppler ratio approach, to those based on Fourier spectrum analysis [7],[8]. Both methods specify that compensation be carried out when aT^2 and vT are greater than thresholds. In the case of the Fourier spectrum analysis, the thresholds define target acceleration and velocity limits above which the Fourier spectrum of the received target signal develops more than one peak. The acceleration and velocity thresholds are respectively ten times and six times smaller for the range and Doppler ratio approach than for the Fourier spectrum approach. These comparisons indicate that the target return can be spread over multiple range-Doppler bins even when the received signal has a single peak in the Fourier power spectrum.

Table 1: Conditions for velocity and acceleration compensation.

Conditions for:	Range/Doppler Ratio	Fourier spectrum
acceleration compensation	$aT^2 > 0.25\lambda$	$aT^2 > 2.5\lambda$
velocity compensation	$vT > 0.5\rho$	$vT > 2.95\rho$

5.3 Effect of velocity and acceleration on detection performance

A comparison of detection performance for different values of velocity and acceleration is carried out by evaluating (9). Consider an S-band example where $\lambda = 0.1$ m, $T = 0.5$ s, $\rho = 40$ m, and $P_{fa} = 10^{-6}$. In order to limit range and Doppler migration, the velocity and acceleration should satisfy $v \leq 40$ m/s and $a \leq 0.1$ m/s^2, according to the conditions given in (10) and (11).

For a fixed acceleration value of 0.1 m/s^2 and velocity values of 0 m/s, 50 m/s, 60 m/s, and 80 m/s, Figure 2a shows probability of detection as a function of SNR. Compared to a 0 m/s target, increasing the target velocity to 50 m/s, 60 m/s and 80 m/s results in a significant degradation in detection performance. Compared to a 0 m/s target, an additional 3.5 dB of SNR is required to detect a 60 m/s target at a given probability of detection. For an 80 m/s target, an additional 4.8 dB of SNR is required.

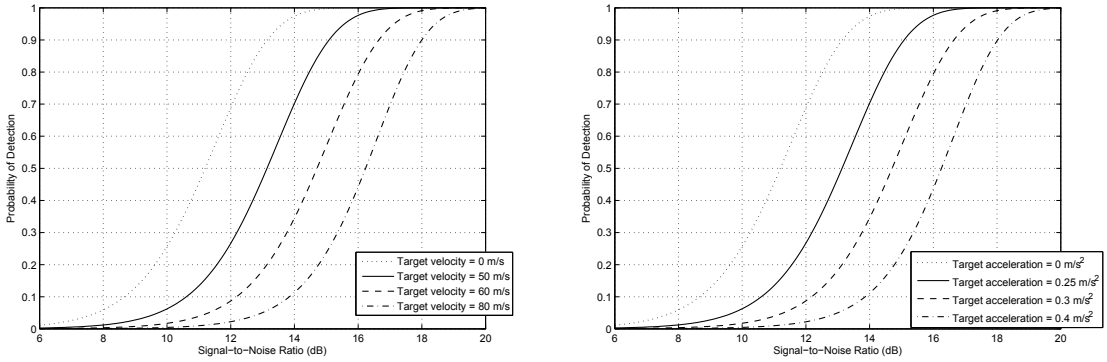

(a) Effect of varying velocity with $a = 0.1$.

(b) Effect of varying acceleration with $v = 40$.

Figure 2: Probability of detection for an S-band example: $\lambda = 0.1$ m, $T = 0.5$ s, $\rho = 40$ m, and $P_{fa} = 10^{-6}$.

Table 2 shows the Doppler and range ratios and the bin count for the various values of target velocity. Doppler ratio Q_d is 0.5 for all cases, since the target acceleration is unchanged at 0.1 m/s^2. The increase in range ratio reflects its linear dependence on velocity. Bin count alone does not indicate detection performance, as the fractional target return power must also be accounted for. For the 50 m/s, 60 m/s and 80 m/s targets, $\gamma = 2$, but the fractional target return powers vary for the three targets and the probability of detection curves in Figure 2a reflect this variation.

For a target velocity of 40 m/s, Figure 2b shows probability of detection for acceleration values of 0 m/s^2, 0.25 m/s^2, 0.3 m/s^2, and 0.4 m/s^2. As acceleration values increase, the degradation in detection performance due to range-Doppler migration is clearly seen. For

Table 2: Ratios and bin count for the S-band example with target acceleration of 0.1 m/s^2.

Target Velocity, m/s	Doppler Ratio Q_d	Range Ratio Q_r	Bin Count γ
0	0.5	0	1
50	0.5	0.625	2
60	0.5	0.75	2
80	0.5	1.0	2

example, compared to a target with no acceleration, an additional 2 dB of SNR is required to achieve a given probability of detection for a target with 0.25 m/s^2 acceleration. For a target with 0.4 m/s^2 acceleration, an additional 5 dB of SNR is required.

The Doppler and range ratios and bin count for varying target acceleration are presented in Table 3. The linear dependence of Doppler ratio Q_d on target acceleration is evident. The increase in Doppler ratio corresponds to the decrease in probability of detection from Figure 2b. In developing the condition to limit range cell migration, it was assumed that in (7) the second term is dominated by the first term. Since the velocity and CPI length are unchanged for all cases in Table 3, any increase in range ratio is due only to an increase in the second term of (7). Results show that this increase is negligible.

Table 3: Ratios and bin count for the S-band example with target velocity of 40 m/s.

Target Acceleration, m/s^2	Doppler Ratio Q_d	Range Ratio Q_r	Bin Count γ
0	0	0.5000	1
0.25	1.25	0.5008	3
0.3	1.5	0.5009	3
0.4	2.0	0.5012	3

5.4 Performance comparison for MIMO Radar

The integration time for MIMO mode is M times longer to compensate for the reduced beam gain across the array. If T_{dir} is the CPI length in Directed Beam mode, then the CPI length for MIMO mode is given by $T_{MIMO} = M\,T_{dir}$. The conditions specified by (10) and (11) have a quadratic and linear dependency on CPI length, respectively. A radar operating in MIMO mode suffers from degraded detection performance as a result of range-Doppler migration, and the degradation is more severe as M increases.

The detection performance of directed beam and MIMO modes can be quantified by evaluating (9). Consider an X-band example where $\lambda = 0.03$ m, $T_{dir} = 0.1$ s, $\rho = 30$ m, $v = 25$ m/s, $a = 0.1$ m/s^2 and $P_{fa} = 10^{-5}$. For the given values of wavelength, range cell length, and CPI length, the velocity and acceleration should satisfy $v \leq 150$ m/s and $a \leq 0.75$ m/s^2 to limit range and Doppler migration. Probability of detection is computed for Directed Beam mode and for MIMO mode with 4, 8 and 12 antenna elements. Figure 3 shows the resulting detection curves.

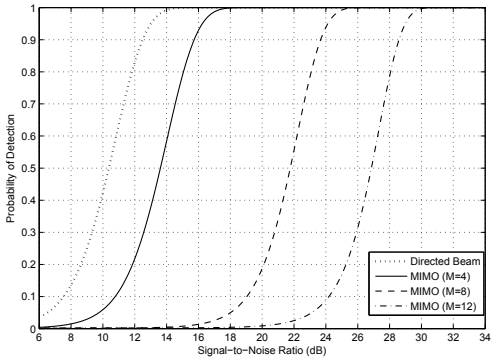

Figure 3: Comparison of MIMO radar performance for an X-band example: $\lambda = 0.03$ m, $T_{dir} = 0.1$ s, $\rho = 30$ m, $v = 25$ m/s, $a = 0.1$ m/s^2, and $P_{fa} = 10^{-5}$.

Further insight into detection performance is gained by examining the Doppler and range ratios and bin count, as shown in Table 4. The linear dependence of range ratio on M and the quadratic dependence of Doppler ratio on M are evident. As the number of antenna elements increases, the increase in Doppler ratio caused by target acceleration is the dominant factor that increases range-Doppler migration. For Directed Beam mode, the bin count is one. For MIMO mode with $M = 12$, the bin count is 11, which results in a 16 dB shift in probability of detection, compared to Directed Beam mode.

Table 4: Ratios and bin count for the MIMO radar X-band example.

Mode	Doppler Ratio Q_d	Range Ratio Q_r	Bin Count γ
Directed Beam	0.067	0.083	1
MIMO ($M = 4$)	1.067	0.334	2
MIMO ($M = 8$)	4.267	0.668	6
MIMO ($M = 12$)	9.600	1.002	11

6 Compensation of range-Doppler migration

In the previous section, it was shown that target velocity and acceleration can cause range-Doppler migration and result in degraded probability of detection. This section considers the compensation of target velocity and acceleration in signal processing, with the aim of reducing range-Doppler migration.

A number of approaches for carrying out compensation of velocity and acceleration have been developed. Among them are time domain approaches such as scaling processing [11], the fractional Fourier transform [12], the chirp-Fourier transform [13] and frequency domain approaches such as the Keystone algorithm [14]. These techniques compensate for the effect of target velocity and acceleration and produce a modified signal that has reduced residual velocity and acceleration effects. The target velocity and acceleration are not known a priori, so a set of compensation velocity values and acceleration values must be chosen.

In this work, the effect of velocity and acceleration compensation is modelled as follows. It is assumed that the velocity and acceleration are less than a fixed maximum velocity v_{max} and maximum acceleration a_{max}, respectively. A set of uniformly spaced compensation velocities is specified as

$$\left\{0, \tilde{v}, 2\tilde{v}, \ldots \left\lceil \frac{v_{max}}{\tilde{v}} \right\rceil \tilde{v} \right\}.$$

A set of uniformly spaced compensation acceleration values is given by

$$\left\{0, \tilde{a}, 2\tilde{a}, \ldots \left\lceil \frac{a_{max}}{\tilde{a}} \right\rceil \tilde{a} \right\}.$$

In this way, the sets of compensation values are entirely specified by the velocity step size $\tilde{v}$ and the acceleration step size $\tilde{a}$. The value from the set of compensation velocities that is closest to the true velocity is chosen and the received signal is compensated for this velocity value. The effective velocity value after compensation is given by

$$v_c = v - i^* \tilde{v},$$

where

$$i^* = \underset{i=1,\ldots,\lceil \frac{v_{max}}{\tilde{v}} \rceil}{\operatorname{argmin}} |v - i\tilde{v}|.$$

The effective acceleration value after compensation is given by

$$a_c = a - j^* \tilde{a},$$

where

$$j^* = \underset{j=1,\ldots,\lceil \frac{a_{max}}{\tilde{a}} \rceil}{\operatorname{argmin}} |a - j\tilde{a}|.$$

In the following, the velocity and acceleration step sizes are specified for full and partial compensation.

6.1 Full compensation

For full velocity compensation, the velocity step size is given by

$$\tilde{v}_{opt} = \frac{\rho}{T}.$$

With this choice of velocity step size,

$$\max|v_c| = \frac{\rho}{2T}.$$

The resulting residual velocity after compensation satisfies (11), which limits range migration effects.

Full acceleration compensation has an acceleration step size given by

$$\tilde{a}_{opt} = \frac{\lambda}{2T^2}.$$

With this choice of acceleration step size,

$$\max|a_c| = \frac{\lambda}{4T^2}.$$

After compensation, the effective acceleration satisfies (10), which limits Doppler migration effects.

For most types of compensation, the received signal must be processed with all possible compensation values. Therefore, the use of full compensation can lead to high computational complexity, especially if the sets of compensation values are large, such as when the maximum velocity and acceleration values are large. This motivates the consideration of partial compensation, where the step sizes are greater.

6.2 Partial compensation

Partial compensation uses larger step sizes than full compensation. As a result, the sets of compensation values are smaller, which reduces computational complexity. In this study, partial compensation step sizes are expressed relative to full compensation step sizes. Specifically,

$$\begin{aligned} \tilde{v}_\mu &= \frac{\tilde{v}_{opt}}{\mu}, \\ \tilde{a}_\psi &= \frac{\tilde{a}_{opt}}{\psi}, \end{aligned}$$

where $0 < \mu \leq 1$ and $0 < \psi \leq 1$. For partial compensation with $\mu = 0.5$ and $\psi = 0.5$, the spacing between compensation values is twice that of full compensation. When $\mu = 1$ and $\psi = 1$, partial compensation is identical to full compensation. The degradation in performance when using partial compensation compared to full compensation will vary with radar and target parameters.

7 Tracking comparison

In this section, the tracking performance of MIMO mode is compared to that of Directed Beam mode. Compared to Directed Beam mode, target detections in MIMO mode will have improved range rate estimation accuracy due to smaller Doppler bin width. However, MIMO mode may suffer from degraded probability of detection due to range-Doppler migration, unless velocity and acceleration compensation is implemented. The effect of these characteristics on tracking performance will be considered by examining an X-band tracking scenario for four distinct cases:

1. Directed Beam mode
2. MIMO mode with full velocity or acceleration compensation
3. MIMO mode with partial velocity or acceleration compensation
4. MIMO mode without compensation

Details of the two-dimensional tracking scenario are as follows. The radar is an 8-element linear array with a length of 2 m and operates at a wavelength of 0.03 m, corresponding to a frequency of 10 GHz. The range cell length is 10 m. A constant-RCS target has an initial range of 100 km from the radar and is located at zero degrees azimuth relative to the center of the linear array. At the initial range of 100 km, the target SNR is 19 dB. The target travels towards the radar for 90 seconds at zero degrees azimuth, with an initial velocity v and a constant acceleration a. For velocity and acceleration compensation, the maximum velocity is $v_{max} = 250$ m/s and the maximum acceleration is $a_{max} = 1.0$ m/s^2. The probability of false alarm is 10^{-5}. For Directed Beam mode, the beamwidth is 0.76 degrees, and the Doppler bin width is 20 Hz. Referring to (2) and (3), the beamwidth in MIMO mode is also 0.76 degrees, while the Doppler bin width is 20/8 = 2.5 Hz.

Starting at time zero, the radar attempts to detect the target at an update interval of two seconds with probability P_d, which is evaluated using (9). The target SNR increases as the target travels towards the radar. If the target is detected, a target measurement vector is generated by adding Gaussian noise to the ground truth. A target measurement vector consists of a range measurement, an azimuth measurement, and a range rate measurement. The standard deviations of the added noise are specified as $\sigma_{\text{range}} = \rho/4$ for the range measurement, $\sigma_{\text{azimuth}} = \theta/4$ for the azimuth measurement, and $\sigma_{\text{range rate}} = \Omega/4$ for the range rate, where ρ, θ and Ω are the range cell length, beamwidth, and Doppler bin width, respectively. The tracker employs an Interacting Multiple Model algorithm [15] that incorporates a constant velocity model and a Singer manoeuvring model for estimating target dynamics. For the target acceleration values under consideration, the constant velocity model consistently had a higher model probability. For the constant velocity model, the process noise spectral densities were specified as $q_x = 0.5$ m^2/s^3 and $q_y = 0.5$ m^2/s^3.

For each scenario where v and a are specified, 500 Monte Carlo runs were generated. At each time instant, the resulting track completeness and track accuracy were averaged over all runs for which a track existed. Track completeness was computed as specified in (1). To measure track accuracy, the root mean-squared error (RMSE) of the estimated position was calculated at each update interval,

$$RMSE_{pos} = \sqrt{\frac{1}{N}\sum_{j=1}^{N} \|\hat{\zeta}_j - \zeta\|^2},$$

where $N = 500$, $\hat{\zeta}_j$ is the track position estimate for Monte Carlo run j, and ζ is the ground truth position.

For the first set of simulation results, the target acceleration was 0.1 m/s^2, and the target velocity was varied from 25 m/s to 250 m/s in increments of 25 m/s. The target acceleration value was chosen to be small enough so that target acceleration would not cause Doppler migration. For the scenario parameters, the velocity step size for full compensation is calculated as $\tilde{v}_{opt} = 25$ m/s so that the set of full compensation velocities is

$$\{0, 25, 50, 75, 100, 125, 150, 175, 200, 225, 250\} \text{ m/s}. \tag{12}$$

MIMO with partial compensation used partial velocity compensation with $\mu = 0.2$ and no acceleration compensation. The partial velocity compensation step size is $\tilde{v}_{0.2} = 125$ m/s, and the set of partial compensation velocities is

$$\{0, 125, 250\} \text{ m/s}. \tag{13}$$

Figure 4 presents detection and tracking results. In Figure 4a, the probability of detection at the initial target range of 100 km is shown. Directed Beam mode has a probability of detection of one for all velocity values. For uncompensated MIMO, probability of detection is 0.15 or less for velocity values of 100 m/s and greater. For MIMO with full compensation, the effective target velocity after compensation is zero, since the velocity values match the compensation velocities shown in (12). As a result, the probability of detection for MIMO with full compensation is one for all velocity values. For MIMO with partial compensation, the effective velocity after compensation is the difference between the true velocity and the nearest compensation velocity. It is seen that probability of detection varies with effective velocity, from a high of 1 when the effective velocity is zero to a low of 0.59 when the magnitude of the effective velocity is 50. Probability of detection will increase as the target moves towards the radar, due to decreasing range. Since the scenario time is fixed at 90 seconds, as velocity increases, the target range at the end of the scenario will decrease.

Tracking results are presented in Figures 4b-4c. Figure 4b shows track completeness for all four cases. Directed Beam and MIMO with full compensation have track completeness

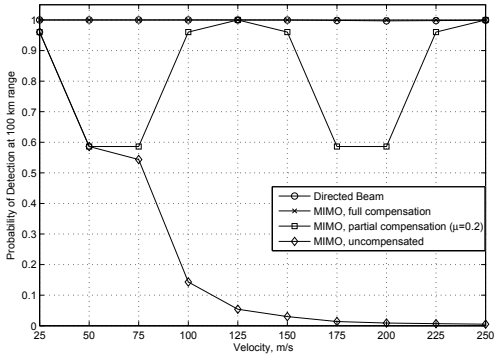

(a) Probability of detection at 100 km range.

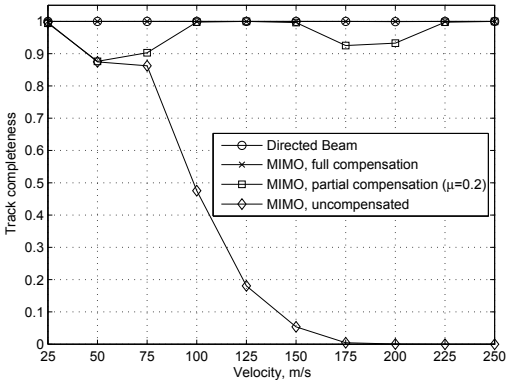

(b) Average track completeness

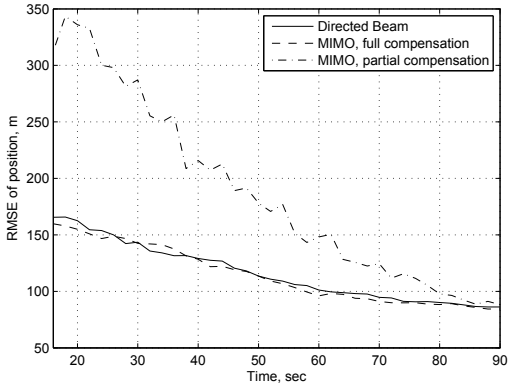

(c) Position RMSE: target velocity of 200 m/s.

Figure 4: Detection and IMM tracking results for X-band scenario with target acceleration of 0.1 m/s^2.

values of essentially one. For both cases, the target is detected at almost every update interval, which updates the track. For MIMO with partial compensation and uncompensated MIMO, track completeness is greater than probability of detection at the initial range. This is mostly due to the ability of the tracker to coast over missed measurements. That is, even when several updates do not produce a measurement, it still may be possible for the tracker to predict a track based on the track history. The increased track completeness relative to probability of detection at the initial range is also partly due to the increase in probability of detection as target range decreases. This effect can be seen in the MIMO with partial compensation case for target velocities of 50 m/s, 75 m/s, 175 m/s, and 200 m/s. For all of these velocities, the initial probability of detection is 0.59, but track completeness increases slightly with velocity.

Figure 4c shows position RMSE for Directed Beam, MIMO with full compensation, and MIMO with partial compensation for a target velocity of 200 m/s. Directed Beam and MIMO with full compensation have essentially the same RMSE. The two modes have probability of detection and track completeness that are essentially one. Although MIMO with full compensation has smaller Doppler bin width, and therefore improved velocity (ie. range rate) estimation accuracy, this has no effect on RMSE. MIMO with partial compensation has larger RMSE than the other two cases. MIMO with full compensation and MIMO with partial compensation have the same velocity estimation accuracy. However, MIMO with partial compensation has smaller probability of detection and coasts over a number of missed measurements. These missed measurements result in increased position RMSE.

For the next set of simulation results, the target velocity was 75 m/s, and the target acceleration varied from 0.1 m/s^2 to 1.0 m/s^2 in increments of 0.1 m/s^2. Full velocity compensation was used for all cases. The acceleration step size for MIMO with full acceleration compensation is $\tilde{a}_{opt} = 0.094$. The set of full compensation acceleration values is

$$\{0, 0.094, 0.188, 0.281, 0.375, 0.469, 0.562, 0.656, 0.750, 0.844, 0.938, 1.031\} \text{ m/s}^2. \quad (14)$$

MIMO with partial acceleration compensation used $\psi = 0.15$. The partial acceleration compensation step size is $\tilde{a}_{0.15} = 0.625$ and the set of partial compensation acceleration values is

$$\{0, 0.625, 1.250\} \text{ m/s}^2. \quad (15)$$

Figure 5a shows probability of detection at the initial range of 100 km. For Directed Beam mode and MIMO with full acceleration compensation, probability of detection is one for all acceleration values. For MIMO with partial acceleration compensation, probability of detection varies between 0.56 and one, and is higher when the true target acceleration is closer to the compensation acceleration values of 0 m/s^2, 0.625 m/s^2 and 1.250 m/s^2.

In Figure 5b, it is seen that track completeness is greater than probability of detection at the initial range, which is due to the ability of the tracker to coast over missed measure-

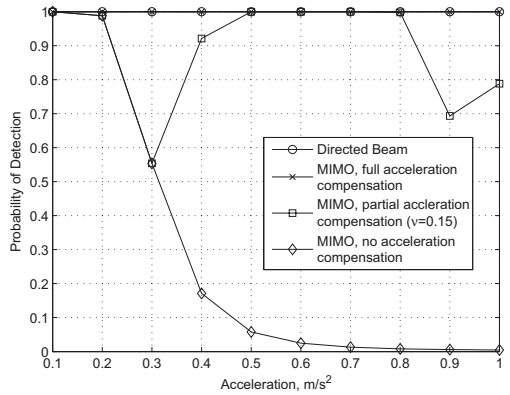

(a) Probability of detection at 100 km range.

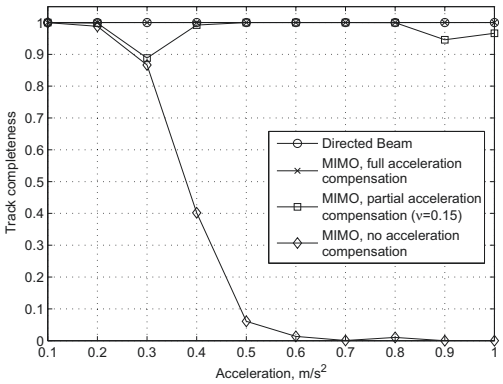

(b) Average track completeness

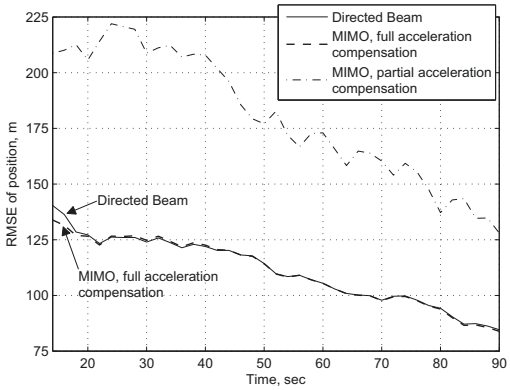

(c) Position RMSE: target acceleration of 0.3 m/s^2.

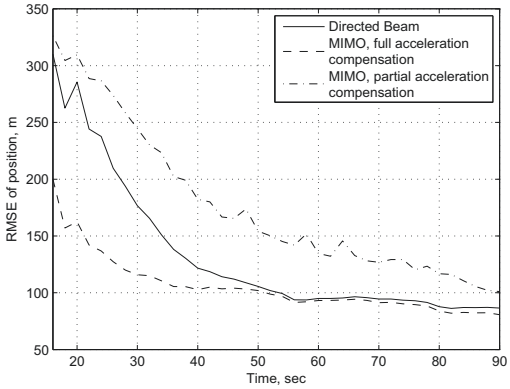

(d) Position RMSE: target acceleration of 0.9 m/s^2.

Figure 5: Detection and IMM tracking results for X-band scenario with target velocity of 75 m/s.

ments. Figure 5c shows the position RMSE for a target acceleration of 0.3 m/s^2. Directed Beam and MIMO with full acceleration compensation achieve essentially the same RMSE, despite the enhanced velocity estimation accuracy of MIMO with full acceleration compensation. MIMO with partial acceleration compensation has larger RMSE than the other two cases due to coasting over missed measurements.

Figure 5d illustrates the position RMSE for a target acceleration of 0.9 m/s^2. MIMO with full acceleration compensation achieves lower RMSE than Directed Beam during the first 50 seconds of the simulation, due to the fact that the improved velocity estimation accuracy of MIMO radar allows the Kalman filter tracker to settle to steady state faster than Directed Beam mode under high target acceleration conditions. The position RMSE of MIMO with partial acceleration compensation is higher than that of MIMO with full acceleration compensation or Directed Beam for the first 50 seconds of the time interval, due to coasting over missed measurements.

8 Conclusions

For a linear array radar, the tracking performance of MIMO mode was compared to that of Directed Beam mode for targets with varying values of velocity and acceleration. MIMO mode requires longer integration times compared to Directed Beam mode which can cause target returns to be spread over multiple range-Doppler bins. An analytical expression for probability of detection that explicitly accounts for range-Doppler migration was derived. Range ratio and Doppler ratio quantify the severity of range-Doppler migration as a function of target velocity, target acceleration, and CPI length. Step sizes for velocity and acceleration compensation were proposed. Full compensation mitigates the effects of range-Doppler migration but has significant computational complexity. Partial compensation has reduced computational complexity but may not completely eliminate the effects of range-Doppler migration.

Single-target tracking performance was analysed for Directed Beam mode, MIMO mode with full compensation, MIMO mode with partial compensation, and uncompensated MIMO mode. For the examples considered, results showed that Directed Beam mode and MIMO with full compensation achieved probability of detection and track completeness close to one. MIMO mode with full compensation had greater positional accuracy than Directed Beam mode for high target acceleration, due to more accurate range rate estimation, but required increased computational complexity as a result of carrying out full compensation. MIMO mode with partial compensation had reduced computational complexity compared to fully compensated MIMO, but suffered from degraded tracking performance due to missed detections which forced the tracker to coast. Uncompensated MIMO mode had low track completeness as velocity and acceleration increased. This poor performance was caused by range-Doppler migration resulting from longer integration times.

This page intentionally left blank.

References

[1] Rabideau, D. and Parker, P. (2003), Ubiquitous MIMO multifunction digital array radar, In *Conference Record of the Thirty-Seventh Asilomar Conference on Signals, Systems and Computers*, Vol. 1, pp. 1057–1064.

[2] Bekkerman, I. and Tabrikian, J. (2006), Target detection and localization using MIMO radars and sonars, *IEEE Trans. Signal Process.*, 54(10), 3873–3883.

[3] Rabideau, D. (2011), Multiple-input multiple-output radar aperture optimisation, *Radar, Sonar Navigation, IET*, 5(2), 155 –162.

[4] Moo, P. (2011), Multiple-input multiple-output radar search strategies for high-velocity targets, *IET Radar Sonar Navig.*, 5(3), 256–265.

[5] Ithapu, V. and Mishra, A. (2009), Hybrid diversity strategy using MIMO radar for target tracking, In *Applied Electromagnetics Conference (AEMC), 2009*, pp. 1 –4.

[6] Gorji, A., Tharmarasa, R., and Kirubarajan, T. (2010), Tracking multiple unresolved targets using MIMO radars, In *Aerospace Conference, 2010 IEEE*, pp. 1 –14.

[7] Yasotharan, A. and Thayaparan, T. (2002), Strengths and limitations of the Fourier method for detecting accelerating targets by pulse Doppler radar, *IEE Proc. Radar Sonar Navig.*, 149(2), 83–88.

[8] Tao, R., Zhang, N., and Wang, Y. (2011), Analysing and compensating the effects of range and Doppler frequency migrations in linear frequency modulation pulse compression radar, *IET Radar Sonar Navig.*, 5(1), 12 –22.

[9] Robey, F., Coutts, S., Weikle, D., McHarg, J., and Cuomo, K. (2004), MIMO radar theory and experimental results, In *Signals, Systems and Computers, 2004. Conference Record of the Thirty-Eighth Asilomar Conference on*, Vol. 1, pp. 300 – 304 Vol.1.

[10] Rice, S. (1944), Mathematical analysis of random noise, *Bell Syst. Tech. J.*, 23, 282–332.

[11] Raney, R., Runge, H., Bamler, R., Cumming, I., and Wong, F. (1994), Precision SAR processing using chirp scaling, *Geoscience and Remote Sensing, IEEE Transactions on*, 32(4), 786 –799.

[12] Almeida, L. (1994), The fractional Fourier transform and time-frequency representations, *Signal Processing, IEEE Transactions on*, 42(11), 3084 –3091.

[13] Xia, X.-G. (2000), Discrete chirp-Fourier transform and its application to chirp rate estimation, *Signal Processing, IEEE Transactions on*, 48(11), 3122 –3133.

[14] Zhu, D., Li, Y., and Zhu, Z. (2007), A Keystone Transform Without Interpolation for SAR Ground Moving-Target Imaging, *Geoscience and Remote Sensing Letters, IEEE*, 4(1), 18 –22.

[15] Blom, H. and Bar-Shalom, Y. (1988), The interacting multiple model algorithm for systems with Markovian switching coefficients, *Automatic Control, IEEE Transactions on*, 33(8), 780 –783.

DOCUMENT CONTROL DATA

(Security markings for the title, abstract and indexing annotation must be entered when the document is Classified or Designated.)

1. ORIGINATOR (The name and address of the organization preparing the document. Organizations for whom the document was prepared, e.g. Centre sponsoring a contractor's report, or tasking agency, are entered in section 8.)

Defence Research and Development Canada – Ottawa
3701 Carling Avenue, Ottawa ON K1A 0Z4, Canada

2a. SECURITY MARKING (Overall security marking of the document, including supplemental markings if applicable.)

UNCLASSIFIED

2b. CONTROLLED GOODS

(NON-CONTROLLED GOODS)
DMC A
REVIEW: GCEC APRIL 2011

3. TITLE (The complete document title as indicated on the title page. Its classification should be indicated by the appropriate abbreviation (S, C or U) in parentheses after the title.)

Tracking performance of multiple-input multiple-output radar for accelerating targets

4. AUTHORS (Last name, followed by initials – ranks, titles, etc. not to be used.)

Moo, P. W.; Ding, Z.

5. DATE OF PUBLICATION (Month and year of publication of document.)	6a. NO. OF PAGES (Total containing information. Include Annexes, Appendices, etc.)	6b. NO. OF REFS (Total cited in document.)
October 2013	40	15

7. DESCRIPTIVE NOTES (The category of the document, e.g. technical report, technical note or memorandum. If appropriate, enter the type of report, e.g. interim, progress, summary, annual or final. Give the inclusive dates when a specific reporting period is covered.)

Technical Memorandum

8. SPONSORING ACTIVITY (The name of the department project office or laboratory sponsoring the research and development – include address.)

Defence Research and Development Canada – Ottawa
3701 Carling Avenue, Ottawa ON K1A 0Z4, Canada

9a. PROJECT OR GRANT NO. (If appropriate, the applicable research and development project or grant number under which the document was written. Please specify whether project or grant.)	9b. CONTRACT NO. (If appropriate, the applicable number under which the document was written.)
11as03	

10a. ORIGINATOR'S DOCUMENT NUMBER (The official document number by which the document is identified by the originating activity. This number must be unique to this document.)	10b. OTHER DOCUMENT NO(s). (Any other numbers which may be assigned this document either by the originator or by the sponsor.)
DRDC Ottawa TM 2012-167	

11. DOCUMENT AVAILABILITY (Any limitations on further dissemination of the document, other than those imposed by security classification.)

(X) Unlimited distribution
( ) Defence departments and defence contractors; further distribution only as approved
( ) Defence departments and Canadian defence contractors; further distribution only as approved
( ) Government departments and agencies; further distribution only as approved
( ) Defence departments; further distribution only as approved
( ) Other (please specify):

12. DOCUMENT ANNOUNCEMENT (Any limitation to the bibliographic announcement of this document. This will normally correspond to the Document Availability (11). However, where further distribution (beyond the audience specified in (11)) is possible, a wider announcement audience may be selected.)

Full unlimited announcement.

13. ABSTRACT (A brief and factual summary of the document. It may also appear elsewhere in the body of the document itself. It is highly desirable that the abstract of classified documents be unclassified. Each paragraph of the abstract shall begin with an indication of the security classification of the information in the paragraph (unless the document itself is unclassified) represented as (S), (C), or (U). It is not necessary to include here abstracts in both official languages unless the text is bilingual.)

Multiple-input multiple-output (MIMO) radar utilizes orthogonal waveforms on each transmit element to achieve virtual aperture extension. Compared to a directed beam radar, MIMO radar has increased Doppler resolution due to longer integration times. However, the requirement for longer integration times can also cause target returns to be spread over multiple range-Doppler bins, which decreases probability of detection. This technical memorandum derives an analytical expression for probability of detection that explicitly accounts for range-Doppler migration. The effect of target velocity, target acceleration and integration time on range-Doppler migration is analysed. A framework for velocity and acceleration compensation and step sizes for full and partial compensation are proposed. Single-target track completeness and track accuracy are computed for four configurations: d irected b eam r adar, M IMO r adar w ith f ull compensation, MIMO radar with partial compensation, and uncompensated MIMO radar. Results indicate that compensation is required to prevent degraded probability of detection as target velocity and acceleration increase. Full compensation mitigates the effects of range-Doppler migration but requires additional computational complexity. The use of partial compensation reduces computational complexity requirements but has diminished tracking performance due to coasting over missed measurements.

Les radars entrée multiple sortie multiple (MIMO) utilisent des formes d'onde orthogonales sur chaque élément émetteur afin de produire une extension virtuelle de leur ouverture. Un radar MIMO a une résolution Doppler plus grande qu'un radar à faisceau dirigé en raison de l'accroissement des temps d'intégration. Cette augmentation des temps d'intégration peut cependant faire en sorte que les échos des cibles s'étendent sur de multiples cellules distance-Doppler, ce qui diminue la probabilité de détection. Le présent document technique développe une expression analytique de la probabilité de détection qui tient explicitement compte de la migration de cellule distance-Doppler. Les effets de la vitesse et de l'accélération de la cible ainsi que du temps d'intégration sur la migration distance-Doppler est analysée. Un cadre de compensation de la vitesse et de l'accélération est proposé ainsi que des grandeurs d'intervalle pour une compensation complète et partielle. L'intégrité et la précision des pistes à une seule cible sont calculées pour quatre configurations : radar à faisceau dirigé, radar MIMO avec compensation complète, radar MIMO avec compensation partielle et radar MIMO sans compensation. Les résultats indiquent qu'une compensation est nécessaire pour empêcher la dégradation de la probabilité de détection lorsque la vitesse et l'accélération de la cible augmentent. La compensation complète réduit les effets de la migration distance-Doppler, mais elle nécessite une complexité de calcul accrue. L'utilisation d'une compensation partielle réduit la puissance de calcul nécessaire, mais elle diminue le rendement de poursuite en raison de mesures manquées qui obligent le radar à avancer à l'aveuglette.

14.

KEYWORDS, DESCRIPTORS or IDENTIFIERS (Technically meaningful terms or short phrases that characterize a document and could be helpful in cataloguing the document. They should be selected so that no security classification is required. Identifiers, such as equipment model designation, trade name, military project code name, geographic location may also be included. If possible keywords should be selected from a published thesaurus. e.g. Thesaurus of Engineering and Scientific Terms (TEST) and that thesaurus identified. If it is not possible to select indexing terms which are Unclassified, the classification of each should be indicated as with the title.)

MIMO Radar
Phased array radar
Radar tracking
Accelerating targets